Inorganic Chemistry

Article

pubs.acs.org/IC

Identifying Nanoscale M_{13} Clusters in the Solid State and Aqueous Solution: Vibrational Spectroscopy and Theoretical Studies

Milton N. Jackson, Jr.,[†] Lindsay A. Wills,[‡] I-Ya Chang,[‡] Matthew E. Carnes,[†] Lawrence F. Scatena,[†] Paul Ha-Yeon Cheong,*[,‡] and Darren W. Johnson*[,†]

[†]Department of Chemistry and Materials Science Institute, University of Oregon, Eugene, Oregon 97403-1253, United States

[‡]Department of Chemistry, Oregon State University, 153 Gilbert Hall, Corvallis, Oregon 97331-4003, United States

Supporting Information

ABSTRACT: Raman spectroscopy, infrared spectroscopy, and quantum mechanical computations were used to characterize and assign observed spectral features, highlight structural characteristics, and investigate the bonding environments of $[M_{13}(\mu_3\text{-}OH)_6(\mu_2\text{-}OH)_{18}(H_2O)_{24}](NO_3)_{15}$ (M = Al or Ga) nanoscale clusters in the solid phase and aqueous solution. Solid-phase Raman spectroscopy was used to reveal that the metal−oxygen (M−O) symmetric stretch (breathing mode) for the Al_{13} cluster is observed at 478 cm^{-1}, whereas this same mode is seen at 464 cm^{-1} in the Ga_{13} cluster. The hydroxide bridges in each cluster are weakly Raman active but show slightly stronger infrared activity. The breathing modes associated with the clusters in the solid state are not clearly visible in aqueous solution. This change in behavior in the solution phase may indicate a symmetry breaking of the cluster or exchange events between protons on the ligands and the protic solvent. Overall, each cluster has several unique vibrational modes in the low wavenumber region (<1500 cm^{-1}) that are distinct from the parent nitrate salt and other polymeric species with similar structure, which allows for unambiguous identification of the cluster in solution and solid phases.

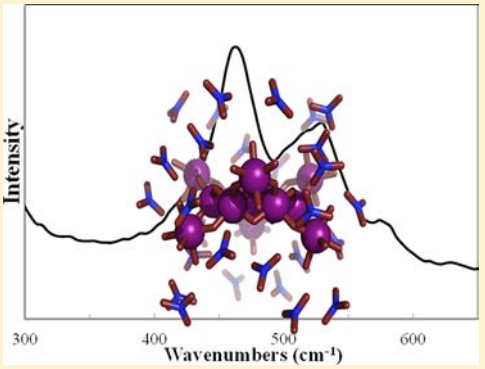

INTRODUCTION

In recent years, the semiconductor industry has increased research efforts toward developing greener and more cost-effective methods of producing thin film devices.[1,2] Group 13 metal aquo-hydroxo clusters with the formula $[M_{13}(\mu_3\text{-}OH)_6(\mu_2\text{-}OH)_{18}(H_2O)_{24}](NO_3)_{15}$ (M = Al or Ga) offer great promise as precursor materials for a variety of applications associated with the fabrication of thin film devices from aqueous solutions.[3,4] However, there is limited knowledge about the growth mechanism, kinetics, solution dynamics, and film formation of these clusters in aqueous solution. To date, there are only a few reported studies on the solution speciation of such clusters.[5−7] A recent study revealed that the Ga_{13} cluster was visible via ^1H NMR in 2 mmol d_6-DMSO.[7] However, because solution-processed thin films are often fabricated in water and at higher concentrations, d_6-DMSO is not an ideal solvent to study for thin film development.[8] As a first step to studying the speciation and solution dynamics in water, this study focuses on characterizing the vibrational modes of the metal clusters in the solid and aqueous solution phase using Raman and infrared spectroscopy − staple techniques which have found limited utility in the characterization of aqueous nanoscale clusters.[9]

The solution speciation and dynamics of these clusters during the spinning, curing, and annealing processes to produce films is of great interest to the material science community as they seek to fine-tune the properties of metal oxide thin films. By identifying and characterizing these clusters in solution, we will be better equipped to monitor the evolution of monomeric Al and Ga species to solution intermediates, then to clusters, and eventually to the production of thin films. By using quantum mechanical computations to assign peaks, we have been able to differentiate between monomeric Al and Ga species and the more complex nanoscale Al_{13} and Ga_{13} clusters in the solid and solution states. This initial study adds to the arsenal of characterization techniques available for studying such aqueous clusters and shows that Raman spectroscopy in particular is an effective reporter of cluster species in solid and solution phases. These studies will provide a baseline for future investigations into understanding cluster formation mechanisms and dynamics/speciation in solution.

EXPERIMENTAL SECTION

1.1. Materials and Sample Preparation. FTIR grade KBr (Aldrich 99.9%) was used in pellet preparation for infrared analysis. $Ga(NO_3)_3{\cdot}xH_2O$ (Aldrich 99.9%) and $Al(NO_3)_3{\cdot}9H_2O$ (STREM 98+ %) were used without further purification as references in both the solid state and the aqueous solution.[7] The Al_{13} cluster was synthesized as previously reported via a zinc reduction method and crystallographically confirmed prior to spectral analysis using single-crystal XRD.[10] As reported previously, zinc acts as a reducing agent, which

Received: March 12, 2013
Published: May 9, 2013

   dx.doi.org/10.1021/ic400611z | Inorg. Chem. 2013, 52, 6187−6192

consumes acidic NO_3^- ions in solution and slowly raises pH. This gradual increase in pH prevents the formation of tetrahedral AlO_4^-, which prevents nucleation of Keggin ions and favors the formation of the flat Al_{13} cluster. Herein, we show that the zinc reduction method can also be extended to form the Ga_{13} cluster as well.

Zn Reduction Method for the Synthesis of $Ga_{13}(\mu_3\text{-}OH)_6(\mu_2\text{-}OH)_{18}(H_2O)_{24}(NO_3)_{15}$. $Ga(NO_3)_3{\cdot}xH_2O$ (2.55 g) was dissolved in 10 mL of 18.2 MΩ H_2O. Zinc powder was then added into the solution in a 2:1 molar ratio of Ga/Zn and the solution was stirred until the zinc was fully dissolved. The solution was then filtered and the filtrate was evaporated until crystals formed. The crystals were then washed with isopropyl alcohol to selectively remove excess $Zn(NO_3)_2$ and $Ga(NO_3)_3$ and yielded ∼57% of the final product. DOSY NMR spectra and single-crystal XRD matched previous reports. In addition, Raman and IR spectra from a previous synthetic preparation were also identical. Stock solutions of the purified samples were prepared using ultrapure 18.2 MΩ H_2O and exhibited no appreciable changes over the duration of the experiment.

1.2. Raman and Infrared Instrumentation. Raman spectra were collected using an Alpha 300S SNOM confocal Raman microscope in a 180° backscattering configuration. A continuous wave pump laser delivered 45 mW of power with an excitation wavelength of 532 nm. A 0.3 m spectrometer equipped with 1800 grooves/mm grating was used to detect stokes Raman scattering and provided a resolution of 1 cm^{-1}. The spectra from each sample were averaged over 2000 accumulations at 0.5 s integration time per scan. The 520.5 cm^{-1} peak of Si was used as an internal standard.

Infrared spectra for both clusters were acquired with a Nicolet 6700 FTIR spectrometer using a KBr pellet. Spectra spanning the range of 400−4000 cm^{-1} were obtained with 64 scans at a resolution of 2 cm^{-1}. Multiple spectra of different sample batches were collected with each technique to ensure reproducibility of the results.

1.3. Computational Methods. All geometry optimizations and absolute energies were computed at the HF/6-31G(d,p) level of theory with the PCM-UFF continuum solvation model for water in Gaussian09.[11] The fundamental frequencies of the nitrate ion vibrations were obtained from literature.[12] To identify the individual vibrational modes, a least squares fitted computed (LSFC) spectrum was created from the computed frequencies as reported earlier.[13] The juxtaposition of the LSFC spectrum to the experimental spectrum enables the association of all of the peaks with specific vibrational normal modes.

■ $Al_{13}(\mu\text{-}OH)_6(\mu\text{-}OH)_{18}(H_2O)_{24}]^{15+}$: RESULTS AND DISCUSSION

2.1. Raman Spectroscopy: Solid Phase. Several weak modes in the Raman spectrum (Figure 1) of Al_{13} from 200 to 2000 cm^{-1} were observed that correspond to the Al−O vibrational modes in the core and shells of the clusters and are summarized in greater detail in Table S6 of the Supporting Information. The peak at 478 cm^{-1} is attributed to the M−O symmetric stretch of the cluster. Quantum mechanical computations reveal several weak modes between 700 and 1200 cm^{-1} for the μ-OH hydroxyl bridges of the cluster including a weak shoulder at ∼1100 cm^{-1}. Though this region is expected for Al−(OH)−Al bridging vibrations, the peaks for the hydroxyl bridges are difficult to distinguish experimentally due to overlap with the NO_3^- vibrations.[14−16] The expected vibrational modes at 721, 1048, 1352, and 1411 cm^{-1} are in good agreement with previous related reports.[14−16] The cluster also exhibited modes at 1641, 3277, and 3470 cm^{-1}, which are attributed to the out-of-plane O−H water bending ($OH_2{\cdots}NO_3^-$), coordinated O−H stretching (Al-ηH_2O), and O−H stretch of disordered (noncoordinated) waters, respectively (Figure S1 of the Supporting Information).[17]

In comparing the spectra of the Al_{13} cluster to that of $Al(NO_3)_3{\cdot}6H_2O$, we discovered that the spectra exhibit some

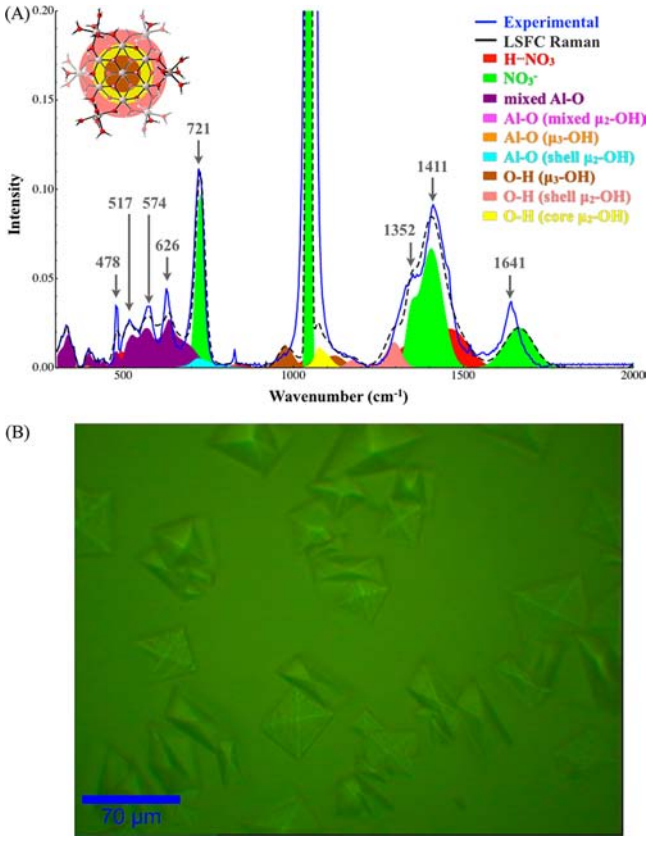

Figure 1. (A) Al_{13} Raman spectrum from 200 to 2000 cm^{-1}. The symmetric stretch of the cluster is highlighted at 478 cm^{-1}. The RMSD for this LSFC Raman spectrum is 0.52%. The colored rings around the cluster inset highlights the three major bonding regions for the cluster: brown = μ_3-OH core, yellow = μ_2-OH core, red = μ_2-OH shell. This color scheme is used for all the figures throughout the article. (B) Confocal Raman imaging of Al_{13} single crystals.

contrasting features. $Al(NO_3)_3{\cdot}6H_2O$ in the solid state contains a single Al−O stretching vibration at 525 cm^{-1} that corresponds to the O_h $Al(H_2O)_6^{3+}$ ion and three weaker modes below 300 cm^{-1} that are indicative of an aluminum nitrato species.[18] The weak shoulder at ∼1100 cm^{-1} in the Al_{13} spectrum is associated with the hydroxide bridges of the cluster and are not present in $Al(NO_3)_3{\cdot}9H_2O$.[18] There are no significant frequency differences in the NO_3^- ion in the Al_{13} and $Al(NO_3)_3{\cdot}9H_2O$ spectra with the exception of a split peak at 1058 cm^{-1}.[17] This suggests that the nitrates in the cluster are not integral to the overall structure and only coordinate to the cluster via hydrogen bonding, which is consistent with the crystal structure.

The Al_{13} cluster, Boehmite (η-AlO(OH)) and Gibbsite ($Al(OH)_3$), share analogous octahedral metal coordination geometries and bridging hydroxides in their crystal structures. In spite of their structural similarities, the Raman spectrum of Al_{13} remains qualitatively different.[19,20] The Raman spectrum of Boehmite is highlighted by a strong Al−O stretching vibration at 360 cm^{-1}, an Al−(OH)−Al deformation at 1071 cm^{-1}, and two weaker O−H modes spanning from 2900 to 3100 cm^{-1}.[21,22] Gibbsite exhibits 12 Al−O modes from 200 to 500 cm^{-1}, 15 Al−(OH)−Al modes from 500 to 1100 cm^{-1}, and four intense and distinct O−H modes from 3300 to 3600 cm^{-1}.[18,19] Whereas some of the reported modes are similar to those found in the cluster, in the region from 400 to 600 cm^{-1}

dx.doi.org/10.1021/ic400611z | Inorg. Chem. 2013, 52, 6187−6192

the Al_{13} cluster exhibits vibrational modes that are distinct from both minerals.

2.2. Infrared Spectroscopy: Solid Phase. IR spectroscopic studies were performed on solid-state samples of the Al_{13} cluster to elucidate information regarding the relationship between vibrational and structural properties (Figure 2). The

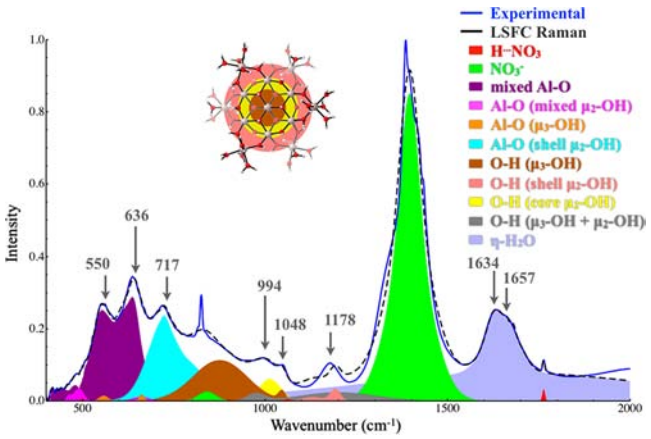

Figure 2. Experimental IR spectra of solid Al_{13} cluster from 400 to 1800 cm^{-1} displaying computational peak analysis. The RMSD for this LSFC IR spectrum is 2.0%. A μ_3-OH ligand is a hydroxide group that bridges the center Al^{3+} with two adjacent core Al^{3+}; μ_2-OH_{core} is a hydroxide group that connects two neighboring core Al^{3+}; μ_2-OH_{shell} is a hydroxide group that links one core Al^{3+} and its closest shell Al^{3+}; and η-H_2O is a terminal water group on the shell Al^{3+}.

O–H bending mode observed at 1660 cm^{-1} is also associated with the exterior waters (η-H_2O) of the Al_{13} cluster that hydrogen bond with the nitrate ions and are consistent with the water deformation mode at 1637 cm^{-1} observed in the Raman spectrum (section 2.1). The modes observed at ~1400 cm^{-1} and 825 cm^{-1} are indicative of the asymmetric and symmetric stretching vibrations of the nitrate ions.[17] Three medium intense Al–O vibrations of the exterior shell vibrations are detected at 500, 620, and 750 cm^{-1}. Smaller weak modes of the bridging hydroxides are observed at 850, 1000, and 1200 cm^{-1} as reported for aluminum-containing minerals.[14−16] A strong, broad O–H absorption band also occurs at 3300 cm^{-1} that represents the water features of the cluster (not pictured in Figure 2, Figures S3 and S6 of the Supporting Information).

The infrared spectrum of the cluster is also different from the respective nitrate salt and mineral. The monomeric species only exhibits a broad Al–O stretch at 600 cm^{-1}, which corresponds to the O_h Al–O stretching vibration of $Al(H_2O)_6^{3+}$.[17] Previous studies on γ-AlO(OH) demonstrated several Al–O modes that have vibrational characteristics similar to those of the Al_{13} cluster.[14−16] However, in contrast to the cluster spectrum, reported values for γ-AlO(OH) highlight various Al–O deformation modes below 400 cm^{-1} as well as Al–O stretching modes at 464, 563, and 626 cm^{-1}. Despite the similarities, it is apparent from the infrared results that the γ-AlO(OH) species forms a different bonding network than Al_{13}. In summary, solid-phase Raman and IR spectroscopy have shown that the Al_{13} cluster exhibits unique vibrational features from its monomeric parent and related polymeric species and both could be used as a viable option for identifying this cluster in the solid state.

2.3. Raman Studies: Solution Phase. Upon dissolution in water, the spectrum of the Al_{13} cluster (Figure 3) reveals that the unique weak vibrational modes featured in the solid state

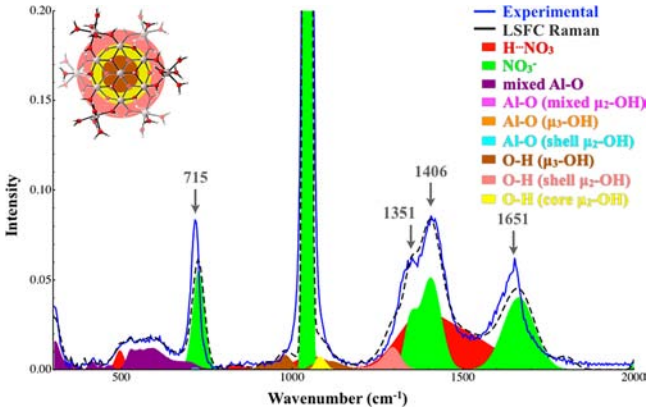

Figure 3. Overlay of simulated (black) and experimental (gray) Raman spectra of Al_{13} in 1 M solution at 25 °C. All of the weak modes seen in the solid phase have merged into one broad feature ranging from 450 to 675 cm^{-1}. The RMSD for this LSFC Raman spectrum is 0.59%.

are no longer distinguishable due to broadening of the vibrational modes into one large feature. The disappearance of these features may indicate a break in symmetry of the cluster, an extended, dynamic hydrogen bonding network with the solvent, or cluster dissociation. The observed Al–O modes are weak and broad, spanning from ~450–675 cm^{-1}. The weak shoulder associated with the hydroxyl bridge at 1100 cm^{-1} is also not observed in the solution spectrum. The water features from 2800 to 3600 cm^{-1} seen in the solid state now resemble bulk water.[23] Upon further inspection, the solution phase Raman spectrum of the cluster is similar to that of aqueous $Al(NO_3)_3$. The only notable difference in the solution phase spectra arises from an increased broadness of the low frequency Al–O stretch associated with the cluster in relation to the narrower octahedral Al–O stretch at 525 cm^{-1} observed in $Al(NO_3)_3$.[17]

The broadness of this peak may result from equilibrium exchange dynamics between the cluster and the solvent that give rise to partial dissociation in solution over time. However, aging the sample shows that this feature remains consistently broad for at least a month. Because the peak does not become narrower with aging to resemble $Al(H_2O)_6^{3+}$, we suspect that the cluster is still present in solution over extended periods of time, consistent with solution DOSY, DLS, SAXS, and related studies on other similar clusters.[7,24] LSFC Raman spectra suggest that Al_{13} and $Al(H_2O)_6^{3+}$ coexist in aqueous solution because the experimental spectrum is best described by a combination of the Al_{13} and $Al(H_2O)_6^{3+}$ species, rather than either species individually (Figure S2 of the Supporting Information). These studies reveal that solution phase Raman spectroscopy provides a complementary technique to determine the full, complex solution speciation of these and related clusters.[25]

■ $[Ga_{13}(\mu_3\text{-}OH)_6(\mu_2\text{-}OH)_{18}(H_2O)_{24}]^{15+}$ RESULTS AND DISCUSSION

3.1. Raman Spectra Analysis: Solid Phase. Raman spectroscopy was also able to provide insight on the vibrational features of the Ga_{13} cluster. A band that appears at 464 cm^{-1} can be attributed to the Ga–O symmetric stretch, or breathing mode, associated with the cluster (Figure 4). Two weaker, but distinct bands of moderate intensity at 525 and 556 cm^{-1} arise

dx.doi.org/10.1021/ic400611z | Inorg. Chem. 2013, 52, 6187−6192

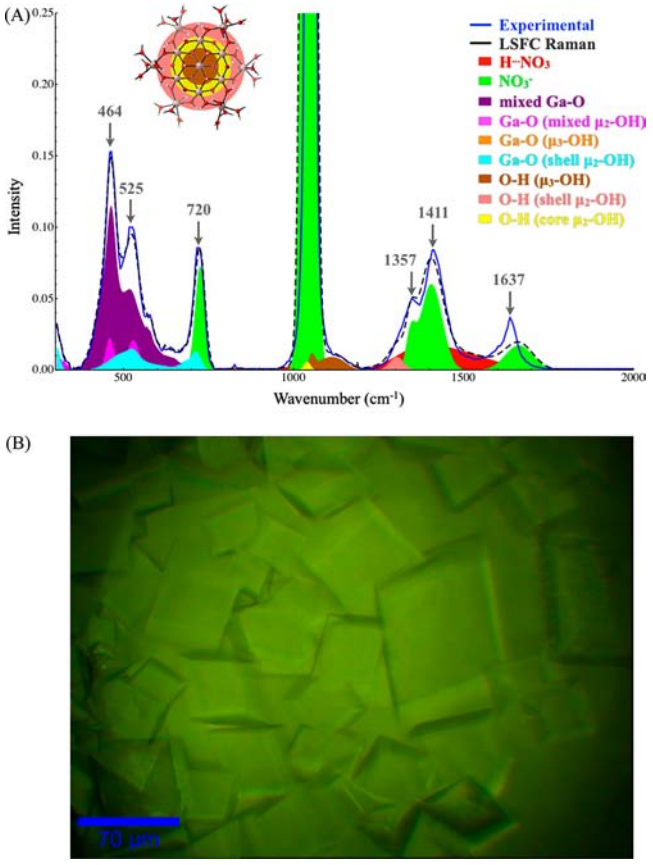

Figure 4. (A) Simulated and experimental Raman spectra from 200 to 2000 cm^{-1} of crystalline Ga_{13} at 25 °C. The feature shown at 464 cm^{-1} arises from the primary breathing mode of the cluster. The RMSD for this LSFC Raman spectrum is 0.40%. (B) Confocal Raman imaging of Ga_{13} single crystals.

from the bending vibrations of the exterior shell of the cluster (Table S7 of the Supporting Information). Calculations suggest that the bands at 1000 and 1100 cm^{-1} can be assigned to the μ_2-OH and μ_3-OH hydroxyl bridges. However, these bands overlap with the symmetric NO_3^- at 1048 cm^{-1} in the same manner as that observed in the Al_{13} cluster. The modes at 720 cm^{-1} and the doublet feature at 1357 cm^{-1} and 1411 cm^{-1} are attributed to the asymmetric nitrate frequencies, which are also present in the Al_{13} cluster (above). Two broad water peaks appear in the traditional O–H stretching region at 3250 and 3425 cm^{-1}. The 3250 cm^{-1} feature can be attributed to tetrahedrally coordinated water molecules with relatively strong hydrogen bonding interactions much like that of H_2O in ice, whereas the 3425 cm^{-1} feature can be assigned to water molecules with hydrogen bonding interactions similar to that of bulk water (Figure S1 of the Supporting Information).[26] A narrow shoulder at 3533 cm^{-1} in the O–H stretching region is also observed and likely due to strongly hydrogen bonded hydroxyl groups incorporated in the crystal lattice of the cluster.[17,26]

Ga_{13}, like Al_{13}, shares similar and contrasting features with $Ga(NO_3)_3{\cdot}xH_2O$. The observed breathing mode of the Ga_{13} cluster at 464 cm^{-1} is significantly lower in energy than the breathing mode of the $Ga(H_2O)_6^{3+}$ species at 525 cm^{-1}.[27,28] This observed energy difference can be attributed to elongation of the bonds in the cluster due to the influence of the extra gallium atoms that make up the cluster. Interestingly, the mode observed at 525 cm^{-1} in the cluster is in the same position as $Ga(H_2O)_6^{3+}$. The similarity most likely arises from the shell of the cluster oscillating in a nearly identical way to the monomer species. The Raman spectrum for $Ga(NO_3)_3{\cdot}xH_2O$ also contains no evidence for bridging hydroxides that are observed in the cluster. Related Raman studies on synthetic nanorods of GaO(OH) identify several strong low energy Ga–O stretching modes around 300 cm^{-1} that are not observed in the Ga_{13} cluster.[29] Additionally, a signature at 605 cm^{-1} in the spectrum of the GaO(OH) species represents a Ga–O stretch of tetrahedral coordination, which is predictably absent in the cluster.[25,26] Because Ga–O bonds in the Ga_{13} cluster spectrum are of pseudo-octahedral coordination, this confirms this distinct coordination geometry of the Ga_{13} cluster.

3.2. Infrared Results: Solid Phase. To complement the results gathered by Raman, IR spectroscopy was also performed on the Ga_{13} cluster in the solid state. Congruent to what was observed by Raman, a broad water absorption that is associated with bulk water occurs at 3359 cm^{-1} (Figure S3 of the Supporting Information). The mode at 1620 cm^{-1} in the IR spectrum of Ga_{13} (Figure 5) is also consistent with the same

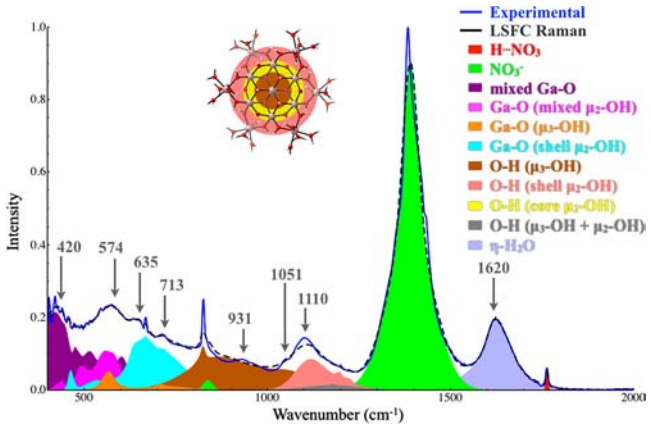

Figure 5. Experimental and simulated IR spectra of Ga_{13} in the solid phase from 400 to 2000 cm^{-1} with computational peak analysis shown. The RMSD for this LSFC IR spectrum is 1.7%.

water out of plane bending mode observed in the Al_{13} IR spectrum (Figure 2) and in the Raman spectra of both clusters (Figures 1 and 4) suggesting that the water in Ga_{13} is interacting with nitrate as previously described for the Al_{13} cluster (section 2.2). The peaks at 824 and ~1381 cm^{-1} are indicative of the asymmetric and symmetric stretching vibrations of the nitrate ion. The bending and stretching vibrational modes of Ga–O in the exterior shell vibrations are detected at 560, 620, and 687 cm^{-1}.

Similar to $Al(NO_3)_3$, $Ga(NO_3)_3$ only contains one weak Ga–O IR signal at 560 cm^{-1}, whereas none of the modes for the hydroxide bridges are present. Smaller weak modes of the μ_x-OH (x = 2 or 3) bridges are observed at 906 and 1102 cm^{-1}. As shown with the Al_{13} cluster, vibrational spectroscopy and computational analysis have given us insight into the vibrational characteristics of the cluster that show Ga_{13} is structurally unique when compared to the parent monomeric gallium nitrate and several oligomeric/polymeric species. However, because of the low intensity of the IR signals for the Ga–O stretch in the Ga_{13} cluster, it may not be the most ideal tool to identify this cluster. In spite of this, it is clear that, with the use of vibrational spectroscopy and quantum mechanical calcu-

dx.doi.org/10.1021/ic400611z | Inorg. Chem. 2013, 52, 6187–6192

lations, we can characterize the Ga_{13} cluster and distinguish it from similar species in solution and the solid state.

3.3. Raman Spectra Analysis: Solution Phase. Upon dissolution, the peaks observed in the solid state decrease and appear as a broad Ga−O stretching vibration centered at 507 cm^{-1} and a shoulder at 450 cm^{-1} (Figure 6). This broadening

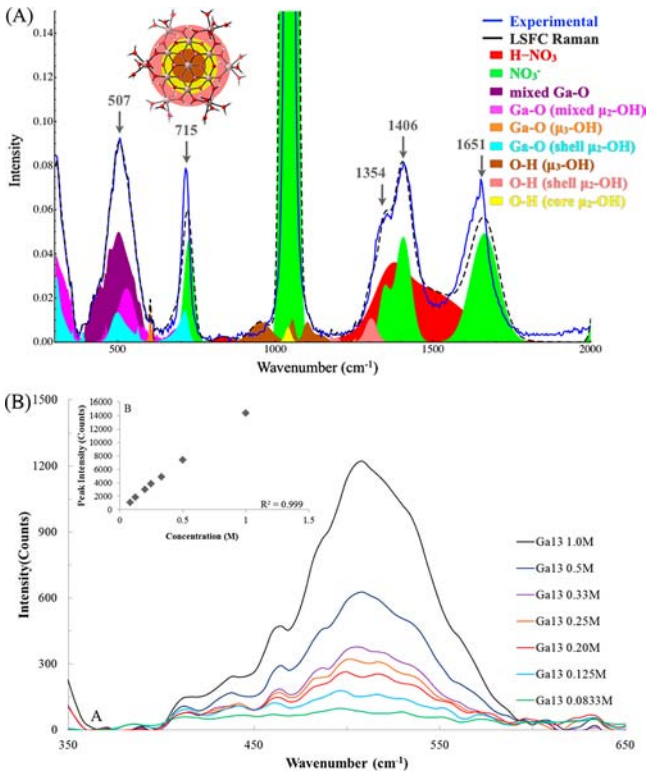

Figure 6. Simulated (A) and experimental (B) Raman spectra of the Ga_{13} cluster in solution phase from 350 to 650 cm^{-1}. The RMSD for this LSFC Raman spectrum is 0.57%. The Ga−O modes coalesce into a broad feature at 502 cm^{-1}. Upon dilution, only the peak intensity changes with dilution suggesting that the species remains persistent in solution (bottom insert). A plot of the intensity of the peak (A) at 502 cm^{-1} vs concentration shows a linear decrease with dilution (B). In spite of the limitations observed with IR, it is clear that, with the use of vibrational spectroscopy, particularly Raman in conjunction with quantum mechanical calculations, we can characterize and identify the Ga_{13} cluster and distinguish it from similar species in solution and the solid state.

phenomenon is very similar to what was observed for the Al_{13}. With increasing dilution, the overall relative intensity of the peaks at 507 cm^{-1} decrease linearly; however, the peak shape remains the same suggesting the dominant species in solution does not change with serial dilution. In comparison to the Ga−O stretch of $Ga(H_2O)_6^{3+}(aq)$ at 525 cm^{-1}, the Ga−O stretch of the cluster at 507 cm^{-1} still vibrates at a slightly lower energy suggesting that Ga_{13} is still present in aqueous solution. This is supported by a previous report showing that the cluster has a size of 5.6 ± 1.8 Å in aqueous solution via small-angle X-ray scattering.[7] As observed with Al_{13}, this feature does not change over the period of a month suggesting potential long-term stability of this species in solution.

■ AL_{13} VS GA_{13}: DISCUSSION

Under the assumption that the outer coordinated waters are treated as point particles, the $M_{13}(\mu\text{-}OH)_6(\mu\text{-}OH)_{18}(H_2O)_{24}^{15+}$ clusters have D_{3d} symmetry. Prior to analysis, we presumed that the clusters would have similar spectra based on the structure and the similar spectroscopic features of their parent nitrate salts.[8,13,14] However, Raman and infrared spectroscopy reveal that the Ga_{13} and Al_{13} clusters have distinct vibrational spectra allowing for definitive characterization and monitoring of cluster species in solution and the solid phase. In the Raman spectra, the observed ν_1 breathing mode for the Al_{13} cluster is observed at 478 cm^{-1}, whereas this same mode occurs at 464 cm^{-1} for the Ga_{13} cluster. This phenomenon is also readily apparent in the IR spectra that reveal that the core and shell hydroxide bridges vibrate at 1110 cm^{-1} for Ga_{13} versus 1178 cm^{-1} for Al_{13}.

In a direct comparison of the Raman spectra of each cluster from 300 to 600 cm^{-1}, the relative intensities of the M−O vibrations in the Ga_{13} cluster spectra are far more intense in the solid state than Al_{13}. In addition, the Al−O bonds in Al_{13} cluster give stronger infrared absorptions as well as more discrete peaks in relation to Ga_{13}. The origins of this phenomenon are complex and could arise from several different factors. One possibility is due to the phenomenon of d-block contraction, Gallium (1.81χ) is more electronegative (Pauling's scale) than aluminum (1.61χ) and the dipole moment (μ) experienced by any specified M−O bond would be greater for Al, which results in greater IR activity. The opposite effect is shown to be true for Ga_{13} in that it is more susceptible to being distorted by an applied electric field (more polarizable) favoring Raman activity. In the solution phase, both polymeric species lose features that are prominent in the crystalline phase resulting in one broad feature because of the additional degrees of vibrational freedom. With dilution, it appears that the Ga_{13} cluster remains present in solution over a wide variety of concentrations and it remains persistent in solution over extended periods of time. However, dilution studies of the Al_{13} cluster were inconclusive due to the weak signal shown in the Raman spectrum.

■ CONCLUSIONS

Raman and infrared spectroscopy, as well as quantum mechanical calculations have been used to characterize Al_{13} and Ga_{13} clusters in the solid and solution phases. Our findings show that these clusters exhibit unique vibrational characteristics that differ from the parent monohydrate salts as well as natural and synthetic minerals that have comparable bonding arrangements. We have also shown that, even though these clusters are analogous to each other, they have very different vibrational characteristics from each other and their parent nitrate salt starting materials. The Al_{13} cluster exhibited several Al−O modes in both Raman and IR spectra but showed more prominent IR activity. The Ga_{13} cluster had more intense Ga−O Raman signals but was not as resolved in the IR spectrum. In solution, both clusters experienced an apparent break in symmetry and many of the peaks observed in the solid phase are no longer observable. The M−O mode for each cluster remains constant over an extended period of time suggesting that both clusters remain the predominant species in solution. In summary, this report reveals that both Al_{13} and Ga_{13} can be identified in the solid state and aqueous solution by vibrational spectroscopy and shows that these clusters are present in H_2O over a long time period suggesting that vibrational spectroscopy is an effective complementary technique to more modern approaches aimed at probing nanoscale structure in solution.[23]

dx.doi.org/10.1021/ic400611z | Inorg. Chem. 2013, 52, 6187−6192

■ ASSOCIATED CONTENT

Supporting Information

Raman spectrum of Al_{13} and Ga_{13} from 2800 to 3600 cm^{-1} displaying the (−OH) vibrations; computational and experimental overlays of the 0.1 M Al_{13} and Ga_{13} solutions; experiment infrared spectra of both clusters from 400 to 4000 cm^{-1}; normalized Raman spectra of solid-state Al_{13} and Ga_{13}; detailed table of vibrational modes and symmetry of both clusters. This material is available free of charge via the Internet at http://pubs.acs.org.

■ AUTHOR INFORMATION

Corresponding Author

*E-mail: dwj@uoregon.edu (D.W.J.), paulc@science.oregonstate.edu (P.H.-Y.C.); URL: http://sustainablematerialschemistry.org.

Notes

The authors declare no competing financial interest.

■ ACKNOWLEDGMENTS

We gratefully acknowledge the NSF Center for Sustainable Materials Chemistry (CHE-1102637) for generous financial support. D. W. J. is a Scialog Fellow of Research Corporation for Science Advancement. P. H.-Y. C. is a Vicki and Patrick F. Stone Scholar of Oregon State University and gratefully acknowledges financial support from the Stone family. L. A. W. is a recipient of the Ken and Lise Hedberg Fellowship at Oregon State University and gratefully acknowledges the financial support provided by this fellowship.

■ REFERENCES

(1) Wilk, G. D.; Wallace, R. M.; Anthony, J. M. *J. Appl. Phys.* **2001**, *89*, 5243.
(2) Mensinger, Z. L.; Wang, W.; Keszler, D. A.; Johnson, D. W. *Chem. Soc. Rev.* **2012**, *41*, 1019.
(3) Rather, E.; Gatlin, J. T.; Nixon, P. G.; Tsukamoto, T.; Kravtsov, V.; Johnson, D. W. *J. Am. Chem. Soc.* **2005**, *13*, 3242.
(4) Mensinger, Z. L.; Gatlin, J. T.; Meyers, S. T.; Zakharov, L. N.; Keszler, D. A.; Johnson, D. W. *Angew. Chem Int. Ed.* **2008**, *47*, 9484.
(5) Bi, Z.; Feng, C.; Wang, D.; Ge, X.; Tang, H. *Colloid Surf., A* **2012**, *407*, 91.
(6) Bi, Z.; Feng, C.; Wang, D.; Ge, X.; Tang, H. *Colloid Surf., A* **2012**, *416*, 73.
(7) Oliveri, A. F.; Carnes, M. E.; Baseman, M. M.; Richman, E. K.; Hutchison, J. E.; Johnson, D. W. *Angew. Chem., Int. Ed.* **2012**, *51*, 10992.
(8) Alemayehu, M.; Davis, J. E.; Jackson, M.; Lessig, B.; Smith, L.; Sumega, J. D.; Knutson, C.; Beekman, M.; Johnson, D. C.; Keszler, D. A. *Solid State Sci.* **2011**, *13*, 2037.
(9) Piszczek, P.; Radtke, A.; Grodzicki, A.; Wojtczak, A.; Chojnacki, J. *Polyhedron* **2007**, *26*, 679.
(10) Wang, W.; Wentz, K. M.; Hayes, S. E.; Johnson, D. W.; Keszler, D. A. *Inorg. Chem.* **2011**, *3*, 9.
(11) Frisch, M. J. et al. *Gaussian 09*; Gaussian, Inc.: Wallingford, CT.
(12) Waterland, M. R.; Kelley, A. M. *J. Chem. Phys.* **2000**, *113*, 6760.
(13) Wang, W.; Chang, I.-Y.; Zakharov, L.; Cheong, P. H.-Y.; Keszler, D. A. *Inorg. Chem.* **2013**, *52*, 1807.
(14) Rudolph, W. W.; Masonb, R.; Pyec, C. C. *Phys. Chem. Chem. Phys.* **2000**, *2*, 5030.
(15) Kloprogge, J. T.; Frost, R. L. *J. Mater. Sci.* **1999**, *34*, 4199.
(16) Kloprogge, J. T.; Frost, R. L. *Spectrochim. Acta, Part A* **1999**, *55*, 163.
(17) Kloprogge, J. T.; Frost, R. L. *J. Mater. Sci.* **1999**, *4*, 4367.
(18) Frost, R. L. *Clays Clay Miner.* **1998**, *46*, 280.
(19) Brühne, S.; Gottlieb, S.; Assmus, W.; Alig, E.; Schmidt, M. U. *Cryst. Growth Des.* **2008**, *8*, 489.
(20) Frenzel, J.; Oliveira, A. F.; Duarte, H.; Heine, T.; Seifert, G. *Z. Anorg. Allg. Chem.* **2005**, *631*, 1267.
(21) Noel, Y.; Demichelis, R.; Pascale, F.; Ugliengo, P.; Orlando, R.; Dovesi, R. *Phys. Chem. Miner.* **2008**, *36*, 47.
(22) Frost, R.; Ruan, H.; Kloprogge, T. *J. Raman Spectrosc.* **2001**, *32*, 745.
(23) Baschenko, S. M.; Marchenko, L. S. *Semicond. Phys., Quantum Electron. Optoelectron.* **2011**, 77.
(24) Oliveri, A. F.; Elliott, E. W., III; Carnes, M. E.; Hutchison, J. E.; Johnson, D. W. *ChemPhysChem* **2013**, in press.
(25) A study has recently been submitted reporting the use of Raman spectroscopy to identify species that are present during the electrochemical formation of Al_{13} in solution; see: Wang, W.; Liu, W.; Chang, I.-Y.; Wills, L. A.; Zakharov, L. N.; Cheong, P. H.-Y.; Boettcher, S. W.; Fang, C.; Keszler, D. A. **2013**, manuscript submitted.
(26) Scatena, L. F.; Richmond, G. L. *J. Phys. Chem. B* **2001**, *105*, 11240.
(27) Rudolph, W. W.; Pye, C. C.; Irmer, G. *J. Raman. Spectrosc.* **2002**, *33*, 177.
(28) Rudolph, W. W.; Pye, C. C. *Phys. Chem. Chem. Phys.* **2002**, *4*, 4319.
(29) Zhao, Y.; Yang, J.; Frost, R. L. *J. Raman Spectrosc.* **2008**, 1327.